Case Studies in Construction Materials 14 (2021) e00513

Contents lists available at ScienceDirect

Case Studies in Construction Materials

journal homepage: www.elsevier.com/locate/cscm

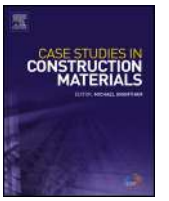

Flexural behavior of HSC one way slabs reinforced with basalt FRP bars

ARTICLE INFO

Article history:
Received 21 December 2020

Keywords:
Baslat fiber reinforced polymer (BFRP) bars
Flexural test
One-way slabs
High Strength Concrete (HSC)
ANSYS 2019-R1

ABSTRACT

This study studied the flexural performance of HSC one-way reinforced concrete slab reinforced with BFRP bars. The study incorporated experimental examination and Non-linear finite element study for seven BFRP concrete slabs had dimensions 700 × 1700 mm with a thickness 120 mm and 140 mm. The experimental test results showed that the ultimate flexural loads and behavior of concrete slabs reinforced with BFRP were improved compared with concrete slabs reinforced with steel reinforcement. Also, the tensile strength of BFRP bar is 2.5 times greater than the yield strength of steel reinforcement and 1.79 times greater than the tensile strength of bar. The structural behavior of the tested slabs was validated with the theoretical developing a finite element models utilize software ANSYS 2019-R1 program. Good agreement between the numerical and experimental results in first cracking loads, load-carrying capacity, crack pattern and deflections were found. The agreement between the experimental load carrying capacity and NLFE ones is about 89.0 % with coefficient of variance equals 0.001 and standard deviation of 0.03. The finite element analysis gave suitable guessing for the structural performance of the nonlinear BFRP concrete slab.

Published by Elsevier Ltd.

1. Introduction

The utilization of FRP for concrete structures exposed to corrosion environment has quickly expanded because of their fantastic resistance to corrosion and high tensile strength. Though, RC members reinforced with FRP bars act in a different way from members reinforced with steel bars. As well, the smaller FRP elastic modulus causes a considerable reduce in the RC members reinforced with FRP bars for flexural stiffness after cracking occur and, thus, bigger deformations in service loading condition. So, designing of RC members reinforced with FRP bars is frequently controlled by serviceability limit state. Hence, using reinforcement of FRP needs an enhanced understanding of the performance of RC members reinforced with FRP bars. Several studies discussed the performance of RC beams and one-way slabs reinforced with various types of FRP bars [1–10] or plastic fibers prepared from recycled polyethylene bottles [11,12]. Though, limited experimental studies on continuously supported RC reinforced beams reinforced with FRP bars had been presented [13–17] and continuous RC slabs reinforced with FRP. Grace et al. [13] examined 7 (two-span) RC T-beams reinforced by CFRP, GFRP and steel bars. This study summarized that beams reinforced with FRP gave the same load carrying capacity like steel RC beams, except different in modes of failure and ductility. Similarly, Razaqpur and Mostofinejad [14] concluded experimental outputs for four continuous RC beams reinforced with CFRP bars and steel stirrups or grid of CFRP for shear requirements. They noticed that grid of CFRP give an equal behavior to steel stirrups. Also, Ashour and Habeeb [15,16] examined simply and continuously RC beams reinforced with CFRP and GFRP bars. They said that continuous RC GFRP beams gave former and wider cracks when comparing with RC steel beams. Additionally, continuous RC GFRP and CFRP beams did not display any considerable load carrying capacity. The research also pointed that the equations of ACI 440 1R-06 be capable of logically load carrying capacity prediction. Lately, El-Mogy et al. [17] informed the experimental results of RC continuous GFRP & CFRP beams. This paper proved that the increase in the GFRP had a great result on decreasing the deflections at mid-span and increasing the load carrying capacity and that was reliable with Habeeb and Ashour [16].

https://doi.org/10.1016/j.cscm.2021.e00513
2214-5095/Published by Elsevier Ltd.

Table 1
Specimens details.

Specimen group	Specimen symbol	Thickness (mm)	Main Reinforcement	RFT. type	RFT. Area (mm^2)
Group I	S1	120	6∅10/m	Steel	471.0
	S2	140	6∅10/m	Steel	471.0
Group II	S3	140	6∅10/m	BFRP	471.0
	S4	120	5∅10/m	BFRP	392.5
	S5	120	5∅8/m	BFRP	251.2
	S6	140	6∅8/m	BFRP	301.5
	S7	120	5∅6/m	BFRP	141.3

FRP RC structures undertake larger deflections and wider crack widths when compared with steel bars. Furthermore, studies studying the crack and deflection behaviors of FRP reinforced concrete components had been performed [20,21]. Al-Sunna et al. [22] said that shear and bond contributed considerably to the deformation of GFRP and CFRP RC members. Pan et al. [23] said that RC FRP beams offered brittle properties, and the deflection and crack were larger than that of steel beams. Noël et al. [24] gave simple modifications for the deflection and crack width equations for improving their accuracy at all reinforcement stress levels within the service range. Up till now, most studies of flexural performance used to modify existing theoretical methods [25,26]. For example, some coefficients had been prepared for modifying Branson's equations in the prediction of deflection in RC FRP structures [26]. Those approaches had been used in several design codes of RC FRP structures [18,19]. Though, current design codes do not yet include any guideline for BFRP reinforcement. In recent years, sequence of studies on the properties of BFRP bars and RC BFRP structures had been performed [27–31].

Some researches attention on strengthening systems like using steel, FRP composites and natural fibers [32,33]. Sen and Reddy [34] had performed experimental study to verify the material properties and the connected fractural mechanisms of composite materials. Rodsin, K. et al. [35] examine the axial compressive performance of ELS concrete confined LC-GFRPs composites. They noticed that all measured models were able to assess the ultimate strength of LC-GFRP confined concrete. The current equations made by Pimanmas et al. [36] were applied to expect the compressive strength and an enhanced relation was future for well compressive strength prediction.

2. Experimental program

This study was carried out in Housing and Building National Research Center (HBNRC), Dokki, Egypt. This investigation was carried out to study the effect of using BFRP bars in reinforcement of HSC one-way slabs. The aim of this study was to estimate the ultimate loads, deflections, cracks, and its propagation and determine the mode of the concrete slabs' failure.

2.1. Experimental study

2.1.1. Tested slabs description

The experimental program consists of two groups of concrete slabs with dimension of 1700 mm length and 700 mm width with different concrete thickness of 120 mm and 140 mm. All slabs specimens have concrete compressive strength of 55 MPa.

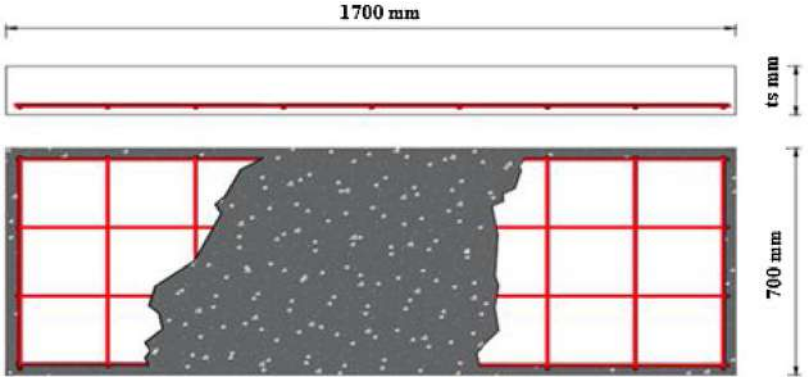

Fig. 1. Dimensions and reinforcement details of the slabs.

Table 2
Concrete Mixes, Materials Weights.

Materials	f_{cu} = 55 MP_a
Silica fume	50
Cement	550
Coarse aggregate	1100
Fine aggregate	590
Water	138
Super-plasticizer	18

Fig. 2. Concrete casted into cubes moulds.

The program consists of two groups of concrete slabs. The first one represents control slabs with thickness of 120 mm and 140 mm reinforced using steel bars of 6 ∅ 10/m [41]. The second group S3 to SP7 reinforced using basalt bars of diameters 6 mm, 8 mm, and 10 mm. The experimental program discussed the effect of several parameter in the concrete slabs such as bars diameters and the slabs thickness. All specimens' details were shown in Table 1 and Fig. 1.

2.1.2. Concrete mix

There was one concrete mix used in the experimental program of compressive strength of 55 MP_a. The materials weights used are presented in Table 2. There were ten concrete cubes were poured during poured the concrete slabs as shown in Fig. 2.

2.1.3. Compressive strength test

Compressive strength test was executed on cube samples of dimensions 150 × 150 × 150 mm. Samples were tested after 7and 28 days. A universal testing machine (2000 kN capacity) was used for the testing as in Fig. 3. The average of the three-tested cubes was expressed the compressive strength as in Table 3.

2.1.4. Basalt bars "BFRP"

BFRP bars were used instead of steel reinforcement. Fig. 4 showed the BFRP bars tensile strength test for different diameters. The test was performed in Housing and Building National Research Center (HBNRC), Dokki, Egypt as in Fig. 5. Basalt bars tensile strength is about 2–3 times tensile strength of reinforcing steel. Table 4 showed the mechanical properties of BFRP bars.

2.2. Test setup

The concrete slabs were tested under two-point load with load distance of 600 mm. The test was performed under a universal testing machine of maximum capacity of 5000 kN as shown in Fig. 6. The Load was incrementally applied on the specimens. LVDTs was used to record the deflection of slabs at mid span. The load was increased until failure and the loads and deflections were recorded.

Fig. 3. concrete cubes and crushing machine of examined mix.

Table 3
Results of the compressive strength test.

Cubes	Compressive Strength (MPa)	
	7 days	28 days
C1	44.2	53.9
C2	47.7	58.2
C3	48.5	56.7
Avg.	**46.8**	**56.3**

3. Experimental results and discussion

The obtained experimental results were presented in terms of ultimate load, deflections, crack pattern, load-deflection curves for tested slabs as follow.

3.1. Slabs experimental failure load

Applying the experimental tests on the one-way slabs recorded the following results. The control group which contains S1 and S2 of reinforced by steel bars of 6Φ10/m with thickness of 120 mm and 140 mm, respectively. Sustained failure load of 192.0 kN and 211.2 kN for S1 and S2, respectively. This due to increase the slab S2 thickness as discussed by Janus, O., et.al [37]. Group II which consist of S3, S4. S5, S6 and S7 have thickness of 140 mm, 120 mm, 120 mm, 140 mm and 120 mm respectively. The basalt bars used in reinforcing this group with different diameters and thickness as given in Table 1. Slab S3 recorded the highest failure load of 239.0 kN, this is due to increase the slab thickness and using basalt bars of high tensile strength. Slab S7 recorded the lowest experimental failure load, due to thikness of concrete slab and the smallest reinforcement ratio of basalt bars. By decreasing ratio of reinforcement of basalt bars and thickness of tested slabs, the

Fig. 4. Ribbed BFRP bars.

Fig. 5. Tensile test of reinforcing bars, a) Basalt FRP bars; b) BFRP bar under tension test.

experimental loads recorded 203.3 kN, 185.5 kN, 207.1 kN and 150.0 kN for S4, S5, S6 and S7, respectively. This is due to the small reinforcement ratio which led to rupture of BFRP bars. Specimen S4 recorded the most enhanced ultimate load with respect to all other specimens due to the thickness of concrete slab and the used small diameter 6Φ10/m of BFRP bars. Table 5 showed the experimental result.

3.2. Crack pattern and mode of failure

Crack pattern of the control slabs S1 and S2 had a compressive strength for concrete 55 MPa, was featured with cracks propagation in tension zone as shown in Fig. 7 while the failure mode was tension failure T.F. The behavior of S3, S5 and S6 are the same while the reinforcement was basalt reinforcement. So, the concrete capacity is still able to carry load but BFRP bars

Table 4
BFRP bars mechanical properties.

Property	Value
Tensile Strength, fu (MPa), for ∅10	900
Ultimate Strain, €u (%), for ∅10	0.022
Tensile Strength, fu (MPa), for ∅8	790
Ultimate Strain, €u (%), for ∅8	0.020
Tensile Strength, fu (MPa), for ∅6	650
Ultimate Strain, €u (%), for ∅6	0.016
Tensile Modulus (Gpa)	40

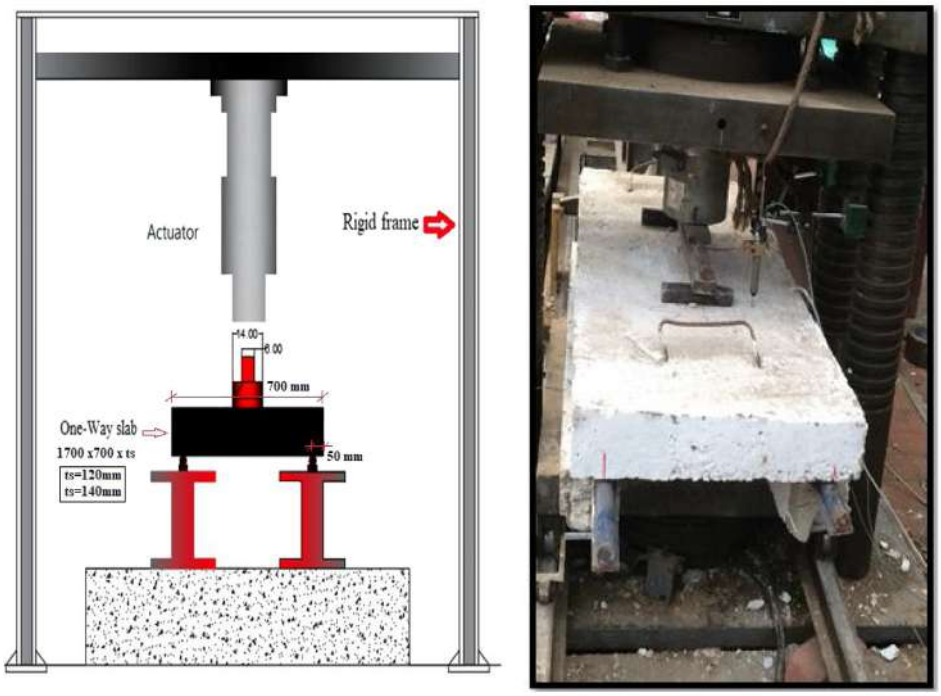

Fig. 6. Specimens details; a) Specimens mold; b) flexural test set up.

Table 5
Experimental obtained results.

Specimen group	Specimen symbol	Thickness (mm)	RFT.	RFT. type	First Crack load (kN)	Ultimate Failure Load (kN)	Ultimate deflection (mm)
Group I	S1	120	6∅10/m	Steel	32.0	192.0	10.4
	S2	140	6∅10/m	Steel	35.0	211.2	11.4
Group II	S3	140	6∅10/m	BFRP	72.0	239.0	7.5
	S4	120	5∅10/m	BFRP	37.0	203.3	11.5
	S5	120	5∅8/m	BFRP	35.0	185.5	12.5
	S6	140	6∅8/m	BFRP	35.0	207.1	13.1
	S7	120	5∅6/m	BFRP	33.0	150.0	14.5

cannot. Rupture occurs in BFRP bars which was sudden rupture so, failure is B.R in bars. For specimens S4 and SP7 the cracks pattern is the same in propagation and mode of failure. The concrete and bars failed together as shown in Fig. 7, mode of failure was occurring of tension cracks and BFRP rupture which attributed to its behavior in failure as shown in Table 6, which with agreed with Zhang, B. et al. [38].

3.3. Deflection of tested slabs

The deflections obtained for all tested slabs were indicated in Table 3. For the group I, the maximum deflation recorded 10.4 mm and 11.4 mm for S1 and S2, respectively. This shows the effect of decreasing the slab thickness in increasing the deflection at the same reinforcement of 6 ∅ 10/m. Specimens S3 and S6 of Group II having the same thickness of 140 mm and the same reinforcement diameter of thickness of 140 mm. It was noticed that the specimens S4 of 6∅ 10/m recorded low deflection of 7.5 mm with respect to the specimen S6 which record 13.1 mm. The load deflection curve for all specimens

shown in Fig. 8. For specimens of thickness 120 mm and 140 mm, load-deflection curves were as shown in Fig. 9a, b. The deflection for S4, S5 and S7 the deflections recorded 11.5 mm, 12.5 mm, and 14.5 mm which agreed with Achillides & Pilakoutas. [39]. The specimens S7 deflection recorded the maximum deflection as shown in Fig. 9b. From Fig. 8, it is obviously notice that the HSC slabs specimens showed linear elastic behavior till failure. Fig. 8 showed that the section acts linear elastic up till the peak load.

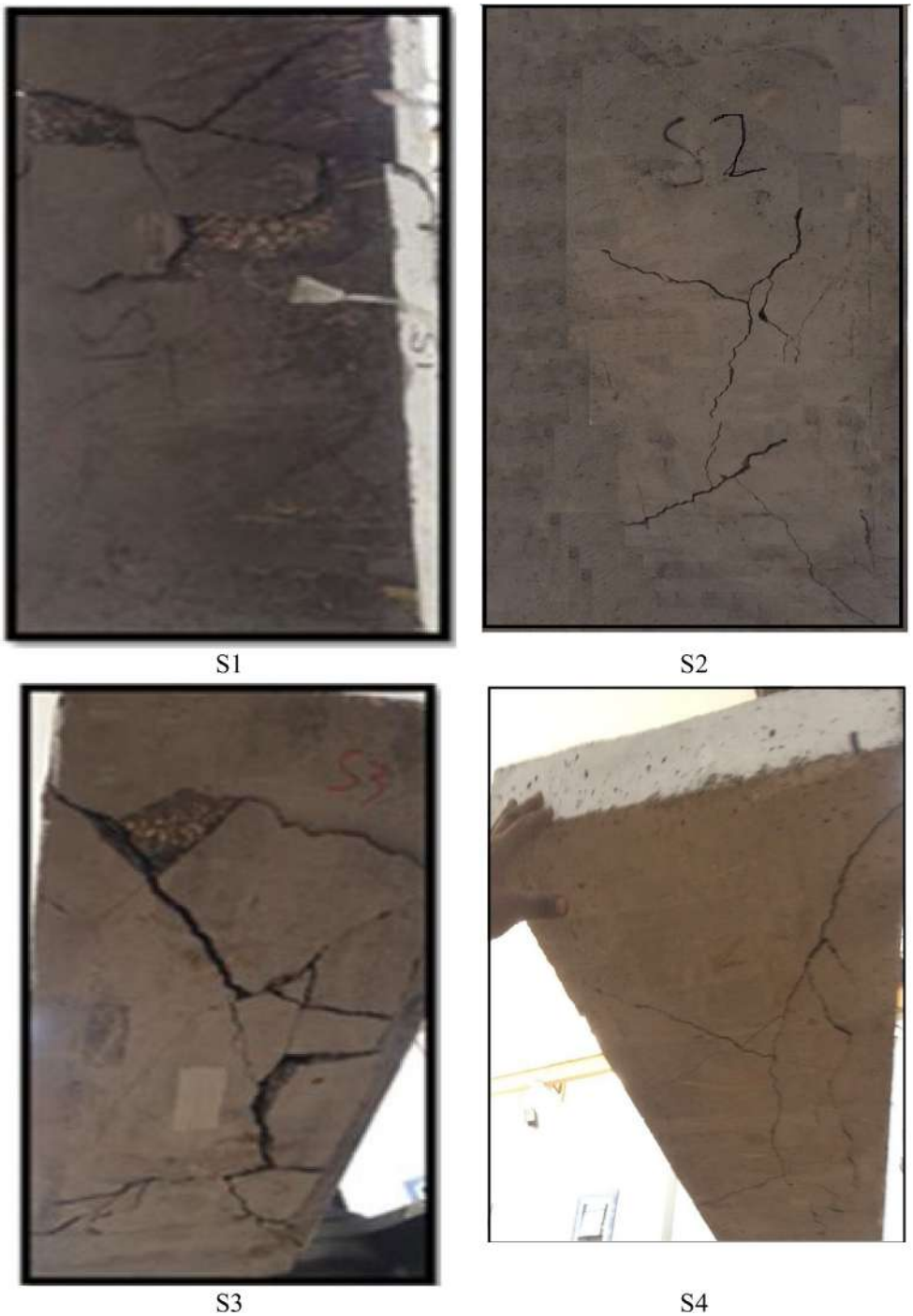

Fig. 7. Cracks Patterns for different Slabs Sample.

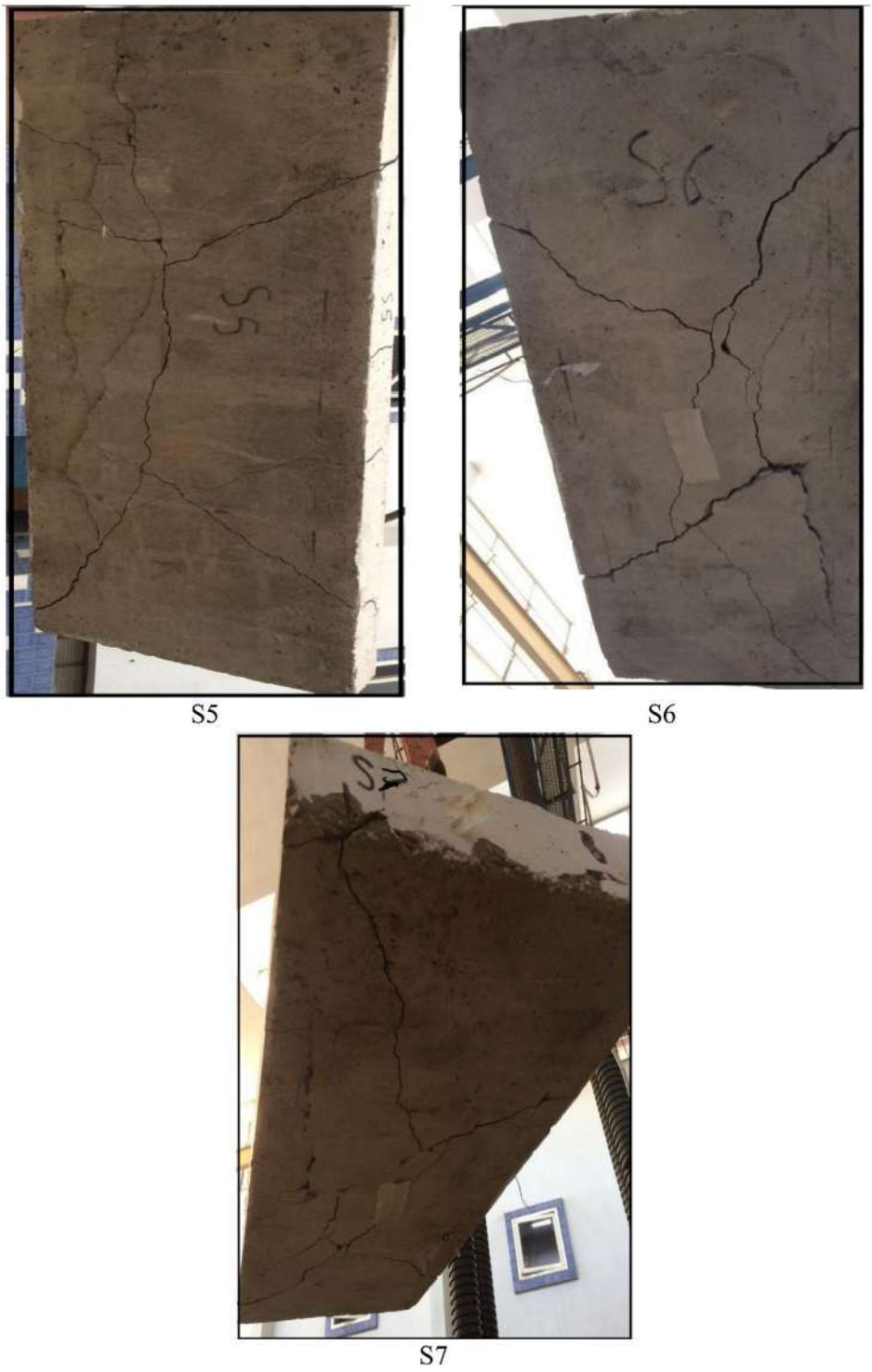

Fig. 7. (Continued)

Table 6
Mode of Failure of Tested One Slabs.

Specimen group	Specimen symbol	Thickness (mm)	Reinforcement	Mode of failure
Group I	S1	120	6∅10/m	T.F
	S2	140	6∅10/m	T.F
Group II	S3	140	6∅10/m	B.R
	S4	120	5∅10/m	C.C.T
	S5	120	5∅8/m	B.R
	S6	140	6∅8/m	B.R
	S7	120	5∅6/m	C.C.T

*T.F tension failure, B.R rupture failure of BFRP bars, C.C.T concrete cracks in tension failure.

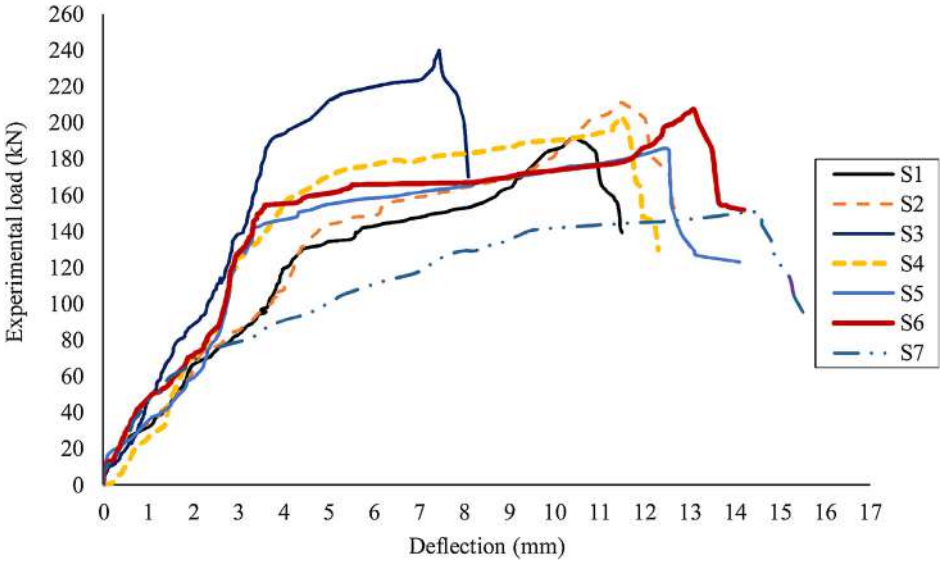

Fig. 8. Load deflection curve for tested slabs.

4. Non-linear finite element analysis

Program of ANSYS 2019-R1 [40] was a finite element model created to commensurate with the experimental program using NLFEA. The analytical study was done to verify the obtained results from the experimental study. The element Solid 65 was used for concrete presentation with mesh size 50 mm and the 3D LINK 180 element was used for presentation of steel & BFRP bars. Fig. 10 showed the geometry and nod locations for elements Solid 65 & LINK 180.

4.1. Verification of model

In this research, the FEA examined cracking, yielding of the steel and failure strength of the slabs. Newton-Raphson method was used for the non-linear response of analysis. Load was increased incrementally till un-convergence which means that failure occurred.

4.2. Material properties

For **concrete**:
Elastic modulus of elasticity: based on ECP 203/2018 [41].
($E_c = 4400\sqrt{f_{cu}} = 24100\ \text{N/mm}^2$)
& Poisson's ratio ($\nu = 0.3$)
For **reinforcing steel** bars: based on ECP 203/2018 [41].

1 Elastic Modulus of elasticity ($E_s = 200\ \text{kN/mm}^2$)
2 Yield stress ($f_y = 360\ \text{N/mm}^2$)
3 Poisson's ratio ($\nu = 0.2$)
4 Area of steel for φ10 ($\text{As} = 78.5\ \text{mm}^2$)

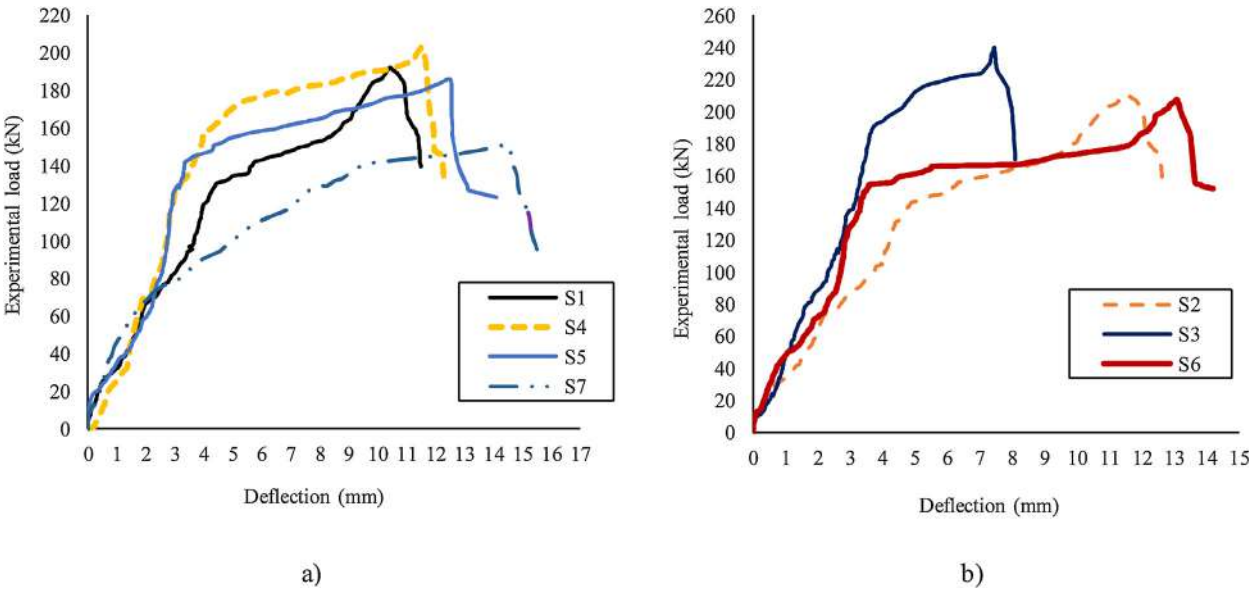

Fig. 9. Load deflection curve; a) specimens of thickness 120 mm, b) specimens of thickness 140 mm.

For **basalt FRP** bars:

1 Elastic Modulus of elasticity (E_f = 40 Gpa)
2 Poisson's ratio (ν = 0.2)
3 Area of BFRP for φ10 (A_f = 78.50 mm^2), Tensile strength (f_u = 900 N/mm^2), ultimate strain (ϵ_u = 0.022).
4 Area of BFRP for φ8 (A_f = 50.30 mm^2), Tensile strength (f_u = 790 N/mm^2), ultimate strain (ϵ_u = 0.020).
5 Area of BFRP for φ6 (A_f = 28.30 mm^2), Tensile strength (f_u = 650 N/mm^2), ultimate strain (ϵ_u = 0.016).

4.3. Modeling

NLFEA was carried out to investigate the flexural behavior of HSC one-way slabs reinforced with BFRP bars ANSYS-2019R1 software as indicated in Fig. 11. The investigated behavior includes the cracks pattern, the ultimate carrying capacity and deflection of the examined slabs.

4.4. NLFE ultimate failure load

The obtained Ultimate loads from analysis were recorded for the one-way slabs of compressive strength of concrete 55 MP_a. Specimen S1 and S2 of the control specimens recorded a failure load $P_{U\ NLFEA}$ of 172.8 kN and 185.9 kN, respectively.

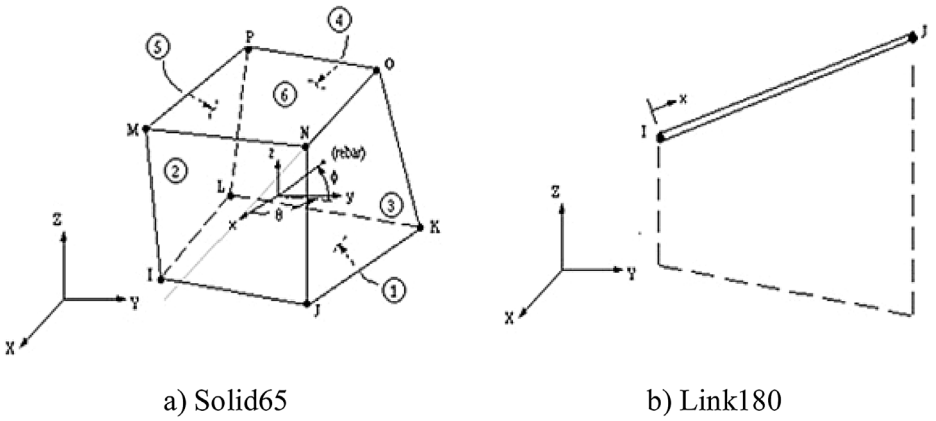

Fig. 10. Geometry & node locations for element types.

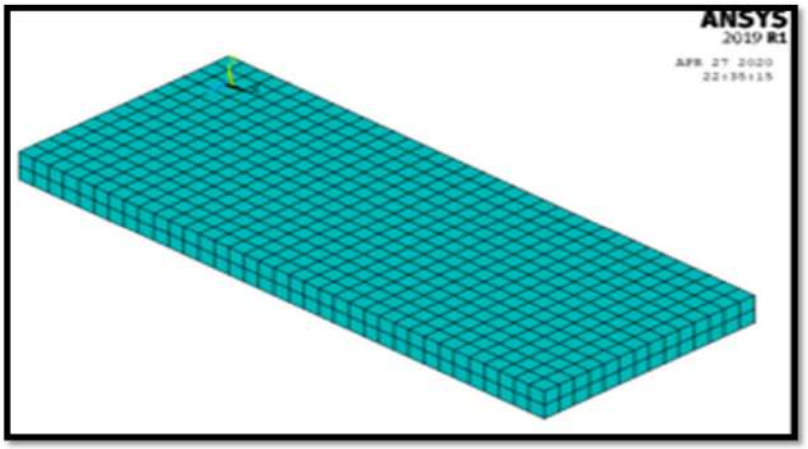

Fig. 11. NLFEA 3D-model of concrete Slabs.

The enhancement in theoretical failure load as same as the experimental behavior manner. The group which used Basalt reinforcement and have the thickness of 140 mm, S3 and S6. The ultimate NLFEA failure loads were 203.2 kN and 190.4 kN, S3 recorded the best failure load with respect to all specimens. For S4, S5 and S7 which have concrete thickness of 120 mm, the theoretical failure load was 182.9 kN, 176.2 kN and 130.5 kN respectively. Slightly enhancement with respect to S1 as shown in Table 7. This indicate that small reinforcement ratio led to rupture of BFRP bars so, failure load decreased as in S7.

4.5. NLFE deflection

The obtained NLFEA deflections were indicated in Table 7. The deflections, generally deflection recorded a good enhancement at the same failure load of control specimens due to using BFRP bars with respect to S1 and S2 reinforced using steel bars.

The deflection of S1 recorded 9.4 mm at failure load but it recorded an enhancement reached to 36.2 % for S3 which recorded the highest failure load. The enhancement was apparent in the load-deflections curves as in Fig. 12.

4.6. Crack pattern

The crack pattern of control group featured with cracks propagation in tension zone as shown in Fig.12a. Also, the failure mode was tension failure T.F due to failure of reinforcement. The behavior of S3 and SP6 were the same slab thickness while the reinforcement was the same in S3 and less than S1 and S2, so the concrete capacity is still able to carry load but BFRP bars cannot. Rupture occurs in BFRP bars which was sudden rupture due to brittle manner of BFRP bars, so failure is R.F in bars. Failure was combination of concrete cracks in compression zone and BFRP bars rupture as in Fig.12b.

5. Comparisons between experimental and NLFEA results

Good agreement obtained between experimental and ANSYS 2019-R1 results by applying a model. The comparisons were applying between failure loads, deflections, the first crack loads.

Table 7
NLFEA Failure Load and Deflections.

Specimen group	Symbol	Thickness (mm)	RFT. type	NLFEA Load (kN)		ΔNLFA (mm)
				First crack	Ultimate load	
Group I	S1	120	Steel	28.0	172.8	9.4
	S2	140	Steel	31.0	185.9	10.03
Group II	S3	140	BFRP	60.0	203.2	6.4
	S4	120	BFRP	31.0	182.9	10.3
	S5	120	BFRP	32.0	176.2	11.9
	S6	140	BFRP	33.0	190.4	12.1
	S7	120	BFRP	29.0	130.5	12.6

5.1. Comparison between experimental and NLFE failure loads

Fig. 13 showed a good agreement between the experimental & NLFEA load capacities PuNLFEA/Puexp. Also, Fig. 13 showed the compatibility between the experimental and analytical load-deflection curves.

The comparisons between the obtained results of different groups of concrete strength 55 MP_a shown in Table 8. The Pu NLFEA/Pu exp. average ratio of 0.89. Group II of concrete reinforced with BFRP of the same concrete thickness but different reinforcement ratios for S3 and S6 respectively, the average was 0.88. Finally, for group of thickness 120 mm and basalt bars with different ratios, the average ratio of agreement for specimens are 0.90. The variance for all specimens were 0.001 and standard deviation of 0.031 showing the effect of using NLFEA in predicting the behavior of the tested specimens as in Table 8 and Fig. 14.

5.2. Comparison between experimental and NLFE deflections

Fig. 15 showed comparison between experimental deflection and NLFEA once until the maximum failure loads. Fig. 15 showed the obtained deflections for all specimens for both experimental and analytical results.

The load deflection curves for tested slabs and analytical results showed a good agreement of an average of agreement of 0.89. Table 8 showed a deflection ratio $\Delta_{u\ NLFEA} / \Delta_{u\ exp.}$ of the control specimens S1 and S2 of 0.90 and 0.88 but for the group reinforcing using the BFRP bar, the ratios were 0.85, 0.89, 0.95, 0.92 and 0.87 for S3, S4, S5, S6 and S7 respectively of an average ratio of agreement was 0.89. This indicate that the analytical models provided an acceptable load deflection response

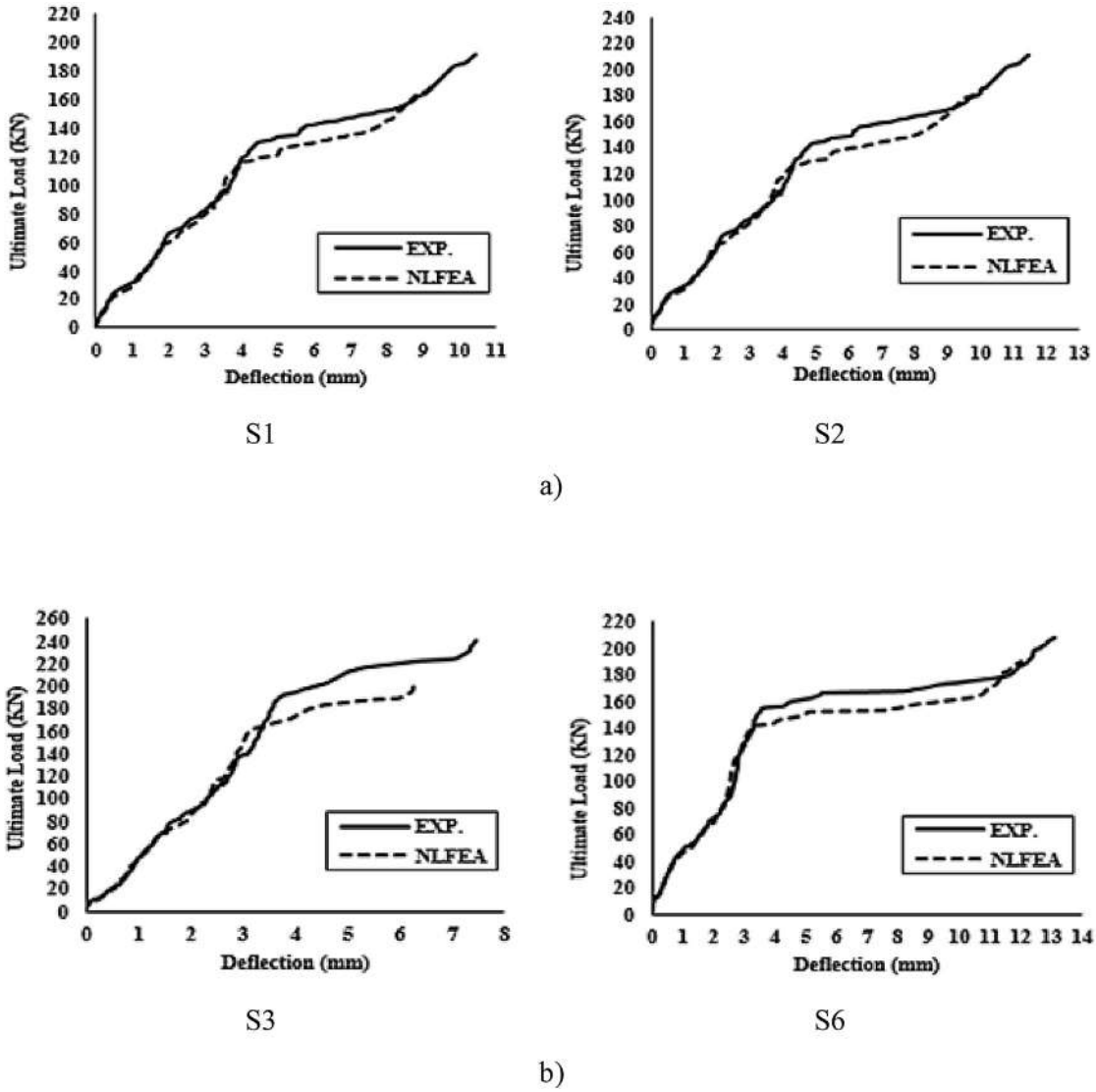

Fig. 12. Load Deflection Curves for Concrete Slabs; A) Control Group S1, S2; B) Slabs of Thickness 140 Mm S3, S6; C) Slabs of Thickness 120 Mm, S4, S5, S7.

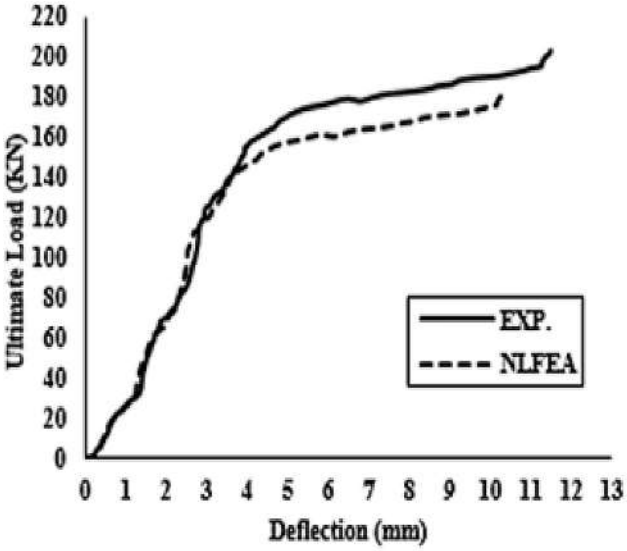

S4

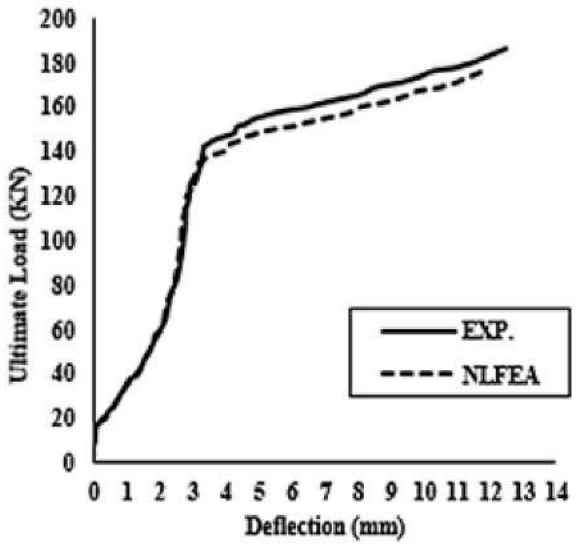

S5

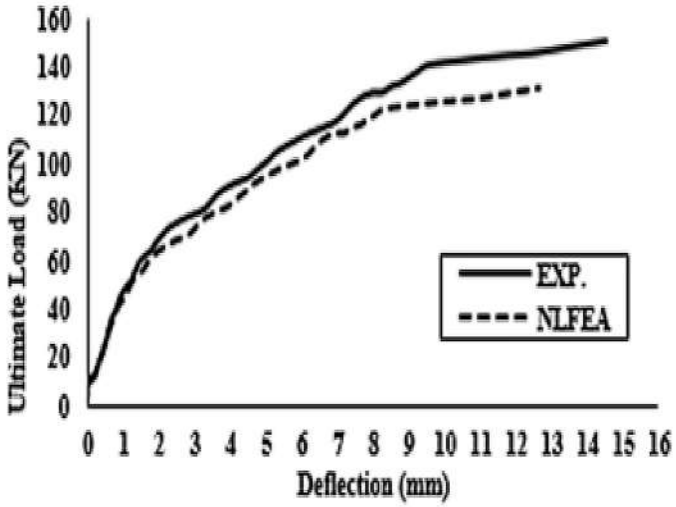

S7

c)

Fig. 12. (Continued)

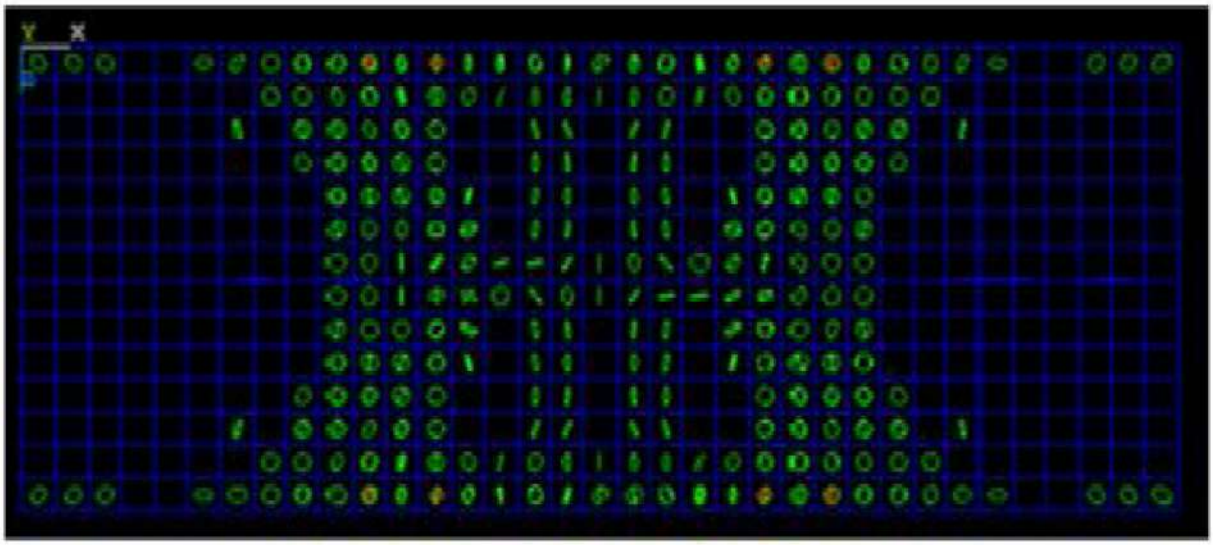

a)

b)

Fig. 13. NLFE Cracks Patterns; a) slabs Reinforced by steel bars; b) slabs reinforced by BFRP bars.

as in Table 8. For all groups, the average of $\Delta_{u\ NLFEA}$ / $\Delta_{u\ exp}$ is equals to 0.89 with a coefficient of variance and standard deviations of 0.001 and 0.031respectively.

5.3. Comparison between experimental and NLFE cracking patterns

The Fig. 16 showed comparison between cracking patterns of cracks obtained from experimental and in nonlinear studies. Cracks started in the form of micro cracks and propagated till failure.

Table 8
Comparisons Between Experimental and NLFEA Results.

Specimen group	symbol	Experimental load (kN)		Analytical load (kN)		Δ (mm)		$\frac{Pu\ (NLFE)}{Pu\ (Exp)}$		$\frac{\Delta(NLFE)}{\Delta\ (Exp)}$
		First crack	Max. load	First crack	Max. load	Δ_{exp}	Δ_{NLFE}	First crack	Max. load	
Group I	S1	32.0	192.0	28.0	172.8	10.4	9.40	0.87	0.9	0.9
	S2	35.0	211.2	31.0	185.9	11.4	10.03	0.89	0.88	0.88
Group II	S3	72.0	239.0	60.0	203.2	7.5	6.4	0.83	0.85	0.85
	S4	37.0	203.3	31.0	182.9	11.5	10.3	0.84	0.89	0.89
	S5	35.0	185.5	32.0	176.2	12.5	11.9	0.92	0.95	0.95
	S6	35.0	207.1	33.0	190.4	13.1	12.1	0.94	0.92	0.92
	S7	33.0	150.0	29.0	130.5	14.5	12.6	0.88	0.87	0.87
Average								0.88	0.89	0.89
Variance								0.0015	0.001	0.001
Standard Deviation								0.037	0.031	0.031

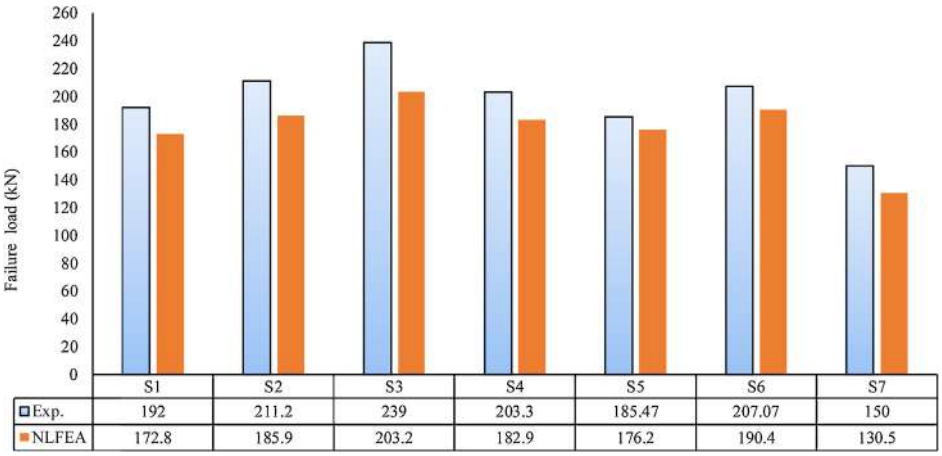

Fig. 14. Comparisons between experimental and NLFE ultimate failure load.

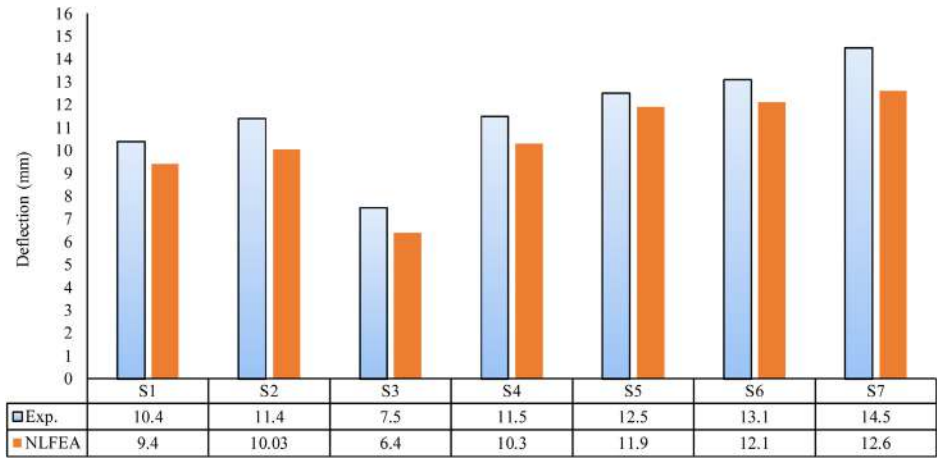

Fig. 15. Comparisons between experimental and NLFE deflections.

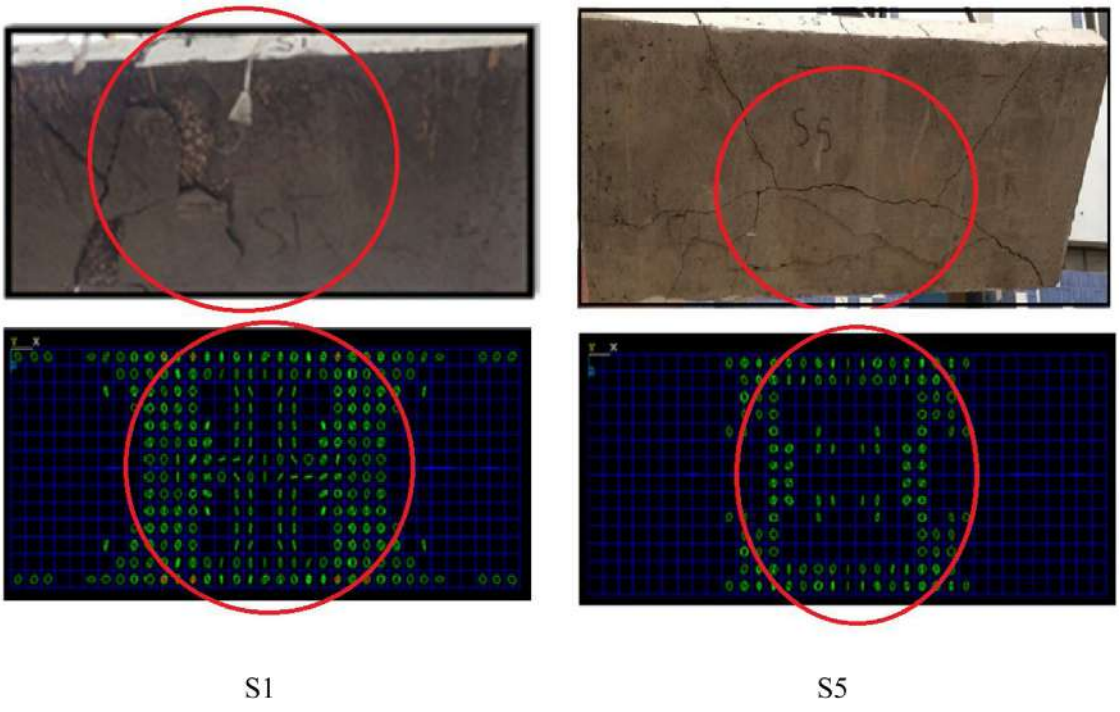

Fig. 16. Cracks Propagation for Slabs S1 and S5.

6. Conclusions

The obtained results and observations of the experimental and the analytical study presented in this thesis were concluding and considering the relatively high variability and the statistical pattern of data. The following conclusions can be drawn:

1 The ultimate flexural loads and behavior of concrete slabs reinforced with BFRP were improved compared with concrete slabs reinforced with steel reinforcement.
2 The tensile strength of BFRP bar is 2.5 times greater than the yield strength of steel reinforcement and 1.79 times greater than the tensile strength of bar.
3 The maximum bond stress values tend to decrease when the embedment length increased for both BFRP bar and steel reinforcement.
4 The maximum bond stress values decrease with increasing bar diameter for both BFRP bar and steel reinforcement.
5 From the slab test results, it has been concluded that the load carrying capacity, concrete compressive strain and tensile bar strain of slabs are increased by increasing the compressive strength of concrete, also the deflections of the slabs were decreased with the addition of fiber to the concrete.
6 The deflections of the slabs were inversely proportional to the amount of the BFRP bars added to the concrete slabs.
7 The behavior of the tested BFRP-reinforced slabs was bilinear elastic until failure. The stiffness of the slabs reinforced with BFRP bars was significantly reduced after initiation of cracks in comparison to the steel-reinforced slabs.
8 There are an enhancement in deflections and the cracks patterns for beams reinforced using BFRP bars especially at equal's reinforcement area.
9 The NLFEA achieved a good agreement with the experimental results varied between 88.0 %–90.0 % in terms of the ultimate loads of the test specimens, first crack load, crack pattern and the deflection at maximum load.
10 The agreement between the experimental load carrying capacity and NLFE ones is about 89.0 % with coefficient of variance equals 0.001 and standard deviation of 0.03.

Declaration of Competing Interest

The authors report no declarations of interest.

References

[1] A.F. Ashour, Flexural and shear capacities of concrete beams reinforced with GFRP bars, Constr. Build. Mater. 20 (2006) 1005–1015.
[2] B. Benmokrane, O. Chaallal, R. Masmoudi, Flexural response of concrete beams reinforced with FRP reinforcing bars, ACI Struct. J. 93 (1996) 46–53.

[3] P.H. Bischoff, Deflection calculation of FRP reinforced concrete beams based on modifications to the existing Branson equation, J. Compos. Constr. 11 (2007) 4–14.
[4] I.F. Kara, A.F. Ashour, Flexure design methodology for concrete beams reinforced with fibre-reinforced polymers, Compos. Struct. 94 (2012) 1616–1625.
[5] H.A. Rasheed, I.R. Naye, H. Melhem, Response prediction of concrete beams reinforced with FRP bars, Compos. Struct. 65 (2004) 193–204.
[6] A.G. Razaqpur, D. Svecova, M.S. Cheung, Rational method for calculating deflection of fiber reinforced polymer reinforced beams, ACI Struct. J. 97 (2000) 175–184.
[7] H. Toutanji, Y. Deng, Deflection and crack-width prediction of concrete beams reinforced with glass FRP rods, Constr. Build. Mater. 17 (2003) 69–74.
[8] H. Toutanji, M. Saafi, Flexure behaviour of concrete beams reinforced with glass fiber-reinforced polymer (GFRP) bars, ACI Struct. J. 97 (2000) 712–719.
[9] P.V. Vijay, H.V.V. GangaRao, Bending behavior and deformability of glass fibre reinforced polymer reinforced concrete members, ACI Struct. J. 98 (2001) 834–842.
[10] J.R. Yost, S.P. Gross, Flexure design methodology for concrete beams reinforced with fibre-reinforced polymers, ACI Struct. J. 99 (2002) 308–316.
[11] D. Foti, Use of recycled waste pet bottles fibers for the reinforcement of concrete, Compos. Struct. 96 (2013) 396–404.
[12] F. Fraternali, I. Farina, C. Polzone, E. Pagliuca, L. Feo, On the use of R-PET strips for the reinforcement of cement mortars, Compos. Part B Eng. 46 (2013) 207–210.
[13] N.F. Grace, A.K. Soliman, G. Abdel-Sayed, K.R. Saleh, Behavior and ductility of simple and continuous FRP reinforced beams, J. Compos. Constr. 4 (1998) 186–194.
[14] A.G. Razaqpur, D. Mostofinejad, Experimental study for shear behavior of continuous beams reinforced with carbon fiber reinforced polymer, Proc., 4th Int. Symp., Fiber Reinforced Polymer Reinforcement for Reinforced Concrete Structures, Farmington Hills, MI: American Concrete Institute, 1999, pp. 169–178.
[15] A.F. Ashour, M.N. Habeeb, Continuous concrete beams reinforced with CFRP bars, Struct. Build. SB6 (2008) 349–357.
[16] M.N. Habeeb, A.F. Ashour, Flexural behavior of continuous GFRP reinforced concrete beams, J. Compos. Constr. 12 (2008) 115–124.
[17] M. El-Mogy, A. El-Ragaby, E. El-Salakawy, Flexural behaviour of FRP-reinforced continuous concrete beams, J. Compos. Constr. 14 (2010) 486–497.
[18] ACI 440.1R-15, Guide for the Design and Construction of Concrete Reinforced with FRP Bars. ACI Committee 440, American Concrete Institute, Farmington Hills, 2015.
[19] CAN/CSA-S6-14, Canadian Highway Bridge Design Code, Canadian Standard Association, Ontario, Canada, 2014.
[20] M. Noel, K. Soudki, Estimation of the crack width and deformation of FRP reinforced concrete flexural members with and without transverse shear reinforcement, Eng. Struct. 59 (2014) 393–398.
[21] A.M. Erfan, H.E. Hassan, K.M. Hatab, T.A. El-Sayed, The flexural behavior of nano concrete and high strength concrete using GFRP, Constr. Build. Mater. 247 (2020) 118664.
[22] R. Al-Sunna, K. Pilakoutas, I. Hajirasouliha, M. Guadagnini, Deflection behaviour of frp reinforced concrete beams and slabs: an experimental investigation, Compos. Part B (Eng.) 43 (5) (2012) 2125–2134.
[23] M.X. Pan, X.S. Xu, Research on deformation characteristics and design method of concrete beams reinforced with GFRP bars, IOP Conference Series: Earth and Environmental Science (2017) 012038.
[24] M. Noël, K. Soudki, Estimation of the crack width and deformation of rereinforced concrete flexural members with and without transverse shear reinforcement, Eng. Struct. 59 (2014) 393–398.
[25] ACI Committee 318, Building Code Requirements for Structural Concrete and Commentary, ACI 318R-05, 2005.
[26] P.H. Bischoff, Reevaluation of deflection prediction for concrete beams reinforced with steel and fiber reinforced polymer bars, ASCE J. Compos. Constr. 131 (5) (2005) 752–762.
[27] J. Shi, X. Wang, Z. Wu, Z. Zhu, Creep behavior enhancement of a basalt fiber reinforced polymer tendon, Constr. Build. Mater. 94 (2015) 750–757.
[28] X. Fan, T. Xu, Z. Zhou, X. Zhou, Experimental study on basic mechanical properties of BFRP bars, Mater. Sci. Eng. Conf. Ser. 250 (1) (2017)012014.
[29] X. Wang, Z. Wu, Evaluation of FRP and hybrid FRP cables for super long-span cable-stayed bridges, Compos. Struct. 92 (10) (2010) 2582–2590.
[30] X. Wang, J. Shi, G. Wu, L. Yang, Z. Wu, Effectiveness of basalt FRP tendons for strengthening of RC beams through the external prestressing technique, Eng. Struct. 101 (2015) 34–44.
[31] Andrzej Garbacz, Marek Urbanski, Andrzej Lapko, BFRP bars as an alternative reinforcement of concrete structures - compatibility and adhesion issues, Adv. Mater. Res. 1129 (2015) 233–241.
[32] Q. Hussain, A. Pimanmas, Shear strengthening of RC deep beams with sprayed fiber-reinforced polymer composites (SFRP): part 2 finite element analysis, Lat. Am. J. Solids Struct. 12 (7) (2015) 1266–1295.
[33] Q. Hussain, A. Ruangrassamee, S. Tangtermsirikul, P. Joyklad, Behavior of concrete confined with epoxy bonded fiber ropes under axial load, Constr. Build. Mater. 263 (2020) 120093.
[34] T. Sen, H.N. Reddy, Efficacy of thermally conditioned sisal FRP composite on the shear characteristics of reinforced concrete beams, Adv. Mater. Sci. Eng. 2013 (2013).
[35] K. Rodsin, Q. Hussain, S. Suparp, A. Nawaz, Compressive behavior of extremely low strength concrete confined with low-cost glass FRP composites, Case Stud. Constr. Mater. 13 (2020) e00452.
[36] A. Pimanmas, Q. Hussain, A. Panyasirikhunawut, W. Rattanapitikon, Axial strength and deformability of concrete confined with natural fibre-reinforced polymers, Mag. Concr. Res. 71 (2) (2019) 55–70.
[37] O. Janus, F. Girgle, V. Kostiha, P. Stepanek, Effect of surface treatment and test configuration on bond behaviour of GFRP rebars, 9th International Conference on Fibre-Reinforced Polymer (FRP) Composites in Civil Engineering (2018) 17–19.
[38] Burong Zhang, Radhouane Masmoudi, Brahim Benmokrane, Behaviour of one-way concrete slabs reinforced with CFRP grid reinforcements, Constr. Build. Mater. 18 (2004) 625–635.
[39] Z. Achillides, K. Pilakoutas, Bond behaviour of fibre reinforced polymer bars under direct pullout conditions, J. Compos. Constr. 8 (2) (2007) 173–181.
[40] ANSYS, "Engineering Analysis System User's Manual" 201, Vol. 1&2, and Theoretical Manual. Revision 8.0, Swanson analysis system inc., Houston, Pennsylvania, 2021.
[41] ECP 208, Egyptian Code of Practice for Design Principles of the Use of Fiber Reinforced Polymers in Construction Permanent Committee, Issued 2018, (2018) .

Abeer M. Erfan
Ragab M. Abd Elnaby
Abdel Aziz Badr
Taha A. El-sayed*,[1]
Department of Structural Engineering, Shoubra Faculty of Engineering, Benha Univeristy, 108 Shoubra Street, Shoubra, Cairo, Egypt
[1] *http://www.bu.edu.eg/staff/tahaibrahim3.*

* Corresponding author. Tel.: +20 1008444985.
E-mail address: taha.ibrahim@feng.bu.edu.eg (T. El-sayed).

Received 21 December 2020